This is a repository copy of *Effects of sucrose on fresh-state and setting properties of air lime*.

White Rose Research Online URL for this paper:
https://eprints.whiterose.ac.uk/203927/

Version: Published Version

Article:

Check for
updates

ORIGINAL ARTICLE

Effects of sucrose on fresh-state and setting properties of air lime

Cecilia Pesce · Giovanni Pesce · Marco Molinari · Marco Corradi

Abstract The use of sustainable additives such as sucrose for improving the properties of lime-based materials can contribute to a wider use of such low-carbon binders with applications in both civil engineering and conservation of the built heritage. Various sucrose-modified lime pastes were prepared, and their microstructure, fresh and hardened properties, and carbonation rate were assessed with an array of analytical techniques. It was found that sucrose acts as a water-reducing agent with relevant effects on both, fresh and hardened properties of pastes while allowing carbonation to occur homogeneously across the whole sample without the formation of carbonation rims. Such effects were enhanced when sucrose was added to the mixture after the slaking as pastes show higher mechanical strength and carbonate at a slower rate. When sucrose was added before the slaking, pastes show high elasticity, low mechanical strength, and carbonate faster due to their fine microstructure.

Keywords Lime · Sucrose · Additives · Carbonation · Microstructure

C. Pesce · G. Pesce (✉)
Department of Architecture and Built Environment, Northumbria University Newcastle, Newcastle upon Tyne NE1 8ST, UK
e-mail: giovanni.pesce@northumbria.ac.uk

M. Molinari
School of Applied Sciences, Huddersfield University, Huddersfield HD1 3DH, UK

M. Corradi
Department of Mechanical and Construction Engineering, Northumbria University, Newcastle upon Tyne NE1 8ST, UK

1 Introduction

One of the biggest challenges to mankind is the adverse effect of climate change, induced by the excess of anthropogenic greenhouse gas (GHG) emissions. The production of Portland cement alone contributes to 3% of the global GHG emissions [1]. Several approaches have been taken to design and introduce low-carbon materials that can satisfy the performance requirements and, at the same time, reduce carbon emissions. Examples are the development of alkali-activated cements and the addition of limestone powder to cement based mixes [2–6]. Another approach is to re-discover traditional materials such as air lime, after they were almost completely abandoned in the twentieth century [7–9]. Air lime is a material of high historical relevance used by mankind since the advent of pyrotechnology over 10,000 years ago [7, 10–13].

However, some characteristics of air lime hinder its wide use in the modern construction industry. These are mainly related to the slow setting rate and the reduced strength compared to other binders [12, 14–17]. Nonetheless, air lime remains particularly attractive as a high quality binder because of its high workability [18], capacity to accommodate movements [17, 19–21], resistance to soluble salts and frost damage [12, 13, 19, 22, 23], breathability [24, 25], self-healing [18, 26] and antiseptic properties [27–29]. Furthermore, the use of lime is already widely regulated, and lime is more environmentally friendly than cement. Upon calcination, lime has reduced CO_2 emissions compared to Portland cement [19, 30, 31] since a substantial part of the emitted CO_2 is re-absorbed while setting. Several new technologies are being developed to replace traditional fossil fuels with alternative sources to operate lime kilns in a more sustainable way. Kilns fuelled with biomass [32–34], hydrogen [33], and solar energy [35] have the potential of making lime production a carbon neutral or even a carbon negative process. Other approaches focus on recycling the emitted CO_2 to be used in the production of carbonated drinks, also with the aim of paying off the environmental costs.

To overcome the limitations of lime, several approaches have been investigated, including the use of lime-cement blends [30, 36, 37], carbonation accelerators [22, 38], and organic additives [16, 39]. The latter holds a great potential for improving lime performance, as the use of organic additive can be not only easily implemented and scalable without the need to considerably change the current technological processes, but also there is a wide range of organic compounds that are stable in atmospheric conditions, non-hazardous, water soluble, affordable and sustainable (since they are by-products of other industrial processes, such as in the case of modified lignosulfonates [40, 41] which are waste products of the wood pulping industry).

Among the additives currently available on the market, sucrose has a long history of use in lime-based mixtures. It was commonly added to Chinese lime mortars [42–46], as well as used in India [47] and Europe during the Greek and Roman periods [48, 49]. Sucrose-based compounds can enhance the mechanical properties and durability of lime pastes and mortars [50–52], and the underlying mechanisms are related to the effects of this molecule on the nucleation and growth of calcium hydroxide crystals [53–56] via complex formation [53, 57] or adsorption/nuclei poisoning mechanism [58]. Sucrose is also a low-cost product, and its production is typically sustainable and efficient [59].

In our previous study [60], we showed that the addition of sucrose is effective in modifying the crystal habit of $Ca(OH)_2$. The resulting sucrose-modified portlandite crystals show characteristics, such as reduced crystallinity and irregular facets, which can influence the carbonation rate. Another recent study [2] showed that sucrose affects the carbonation rate and improves the mechanical performance of mortars made with air lime. Furthermore, it has been suggested that sucrose can affect the carbonation of calcium hydroxide by promoting and stabilising the formation of amorphous calcium carbonate, and eventually leading to the formation of elongated chain-like calcite agglomerates [61]. However, despite these advantages, a comprehensive assessment of the effects of sucrose on the performance of lime-based mixtures is not available yet. One of the aspects that has not been investigated is the optimal method to introduce sucrose into a lime mixture. The aim of this study is to assess the effects of sucrose additions on the fresh and hardened properties of lime pastes, and on their carbonation by adding the sucrose before and after the slaking process.

2 Materials and methods

2.1 Materials

We used commercial quicklime *Calbux Fine 6*, 92% purity, supplied by Tarmac Buxton Lime (UK) and classified as CL90 according to BS EN 459-1 [62], with nominal particle size < 6 mm. The microstructure, mineralogy and chemical composition of the quicklime used were provided in a previous study [60]. The sucrose used was a reagent grade ≥ 99.0% product supplied by Sigma-Aldrich (product code 84,100-1 KG). The marble powder used for the production of the pastes was the commercial product Fordacal Filler Powder (Marble Powder) supplied by MB Fibreglass. Its mineralogical composition determined by X-ray diffraction (Fig. 1) consists of 98% calcite and 2% dolomite.
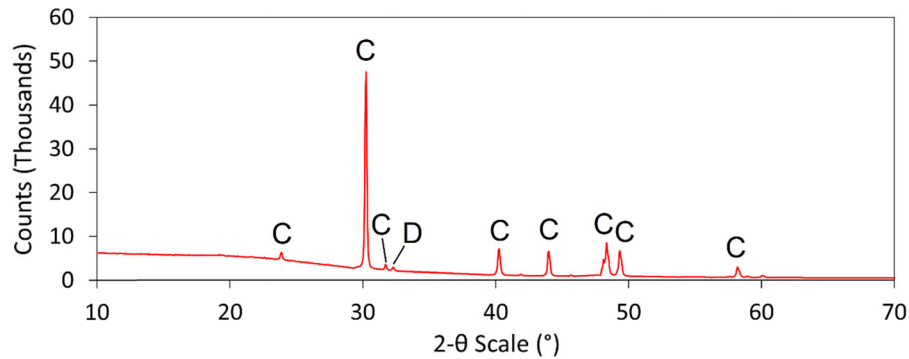
Fig. 1 XRD diffractogram of the marble powder used to produce the tested pastes. Keys: *C* calcite; *D* dolomite

2.2 Sample preparation

Three lime pastes (S1, S2 and control) were produced by mixing sucrose-modified lime putties and a plain lime putty with 30 wt% marble powder. This is a lime-rich mixture similar to the so called 'fat' *marmorino* Venetian plaster [63] that can limit the development of cracks induced by drying shrinkage in lime-based mixtures without substantially affecting the carbonation of lime (details of the mixes are shown in Table 1). The control paste was produced by using a plain lime putty, prepared by placing 1 kg of quicklime into a metal bucket where deionised water was added all at once in a weight ratio oxide:water 1:3, as used in previous studies [58, 64–66]. After the initial bubbling, the slurry was hand-mixed for at least 10 min and subsequently mechanically combined with the marble powder for 5 min using a planetary mixer as specified in EN 196-1 [67]. Paste S1 was produced in a similar way to the control, using a lime putty slaked in a 5% wt sucrose solution. The aqueous solution was prepared by mixing sucrose as received with deionised water until the additive was fully dissolved. Paste S2 was produced using a lime putty that was slaked first in deionised water, and after 10 min of hand-stirring, the solid sucrose was added to the putty as received, in the same concentration as in S1. The water content was calculated by gravimetry after oven-drying a sample of the pastes at 80 °C until constant weight was reached. It can be noted in Table 1 that despite having used the same lime-to-water ratios for all the pastes, S2 shows a lower water content. This is likely due to the fact that the percent water content also takes into account the amount of sucrose contained in the mix, therefore lowering the relative water content. Differently, the S1 paste shows a similar percent water content to the control likely because of the slower, less vigorous slaking reaction that takes place in a sugary solution, as observed empirically by the authors and also reported by Kang et al. [2]. This is likely to lead to a lower slaking temperature and less water evaporation, therefore resulting in a similar, slightly higher than the control, water content despite the presence of sucrose in the mix.

Table 1 List and composition of the tested pastes and relative water content

Sample	Binder	Aggregate	Water content (wt%)
Control	Plain lime putty slaked in deionized water	Marble powder (30% wt)	37.5
S1	Lime putty slaked in 5% wt sucrose solution		38.2
S2	Lime putty slaked in deionized water with addition of solid sucrose after slaking		33.2

2.3 Fresh-state properties

Flowability, dynamic viscosity and water retention were investigated as characteristics of the fresh pastes. The paste flowability was measured through the slump test using a flow table as described in EN 12350-5:2019 [68]. The dynamic viscosity was measured using a handheld vibrational viscometer Hydramotion Viscolite 700 (model VL7-100B-d15). The viscosity value was noted after at least 20 s from probe immersion, while stirring the paste to stabilise the measurements, and the averaged value of 7 readings was considered to obtain a stable reading as recommended by the instrument user manual [69]. The water retention of fresh pastes was investigated using the method detailed in EN 459-2:2010 [70], previously used by other researchers [71], and the testing equipment provided by Novanna Measurement Instrument (product code 1.0246). Three replicas of each test were performed.

2.4 Hardened-state properties

For the hardened-state properties, the fresh pastes were first cast into two sets of moulds: a set of prismatic moulds $40 \times 40 \times 60$ mm with at least 8 specimens per type of paste (Control, S1 and S2) prepared to account for any possible preparation problem (e.g. shrinkage cracks), and a set of cylindrical moulds of 40 mm diameter and 50 mm height with at least 6 specimens per type of paste. All samples were placed into a ventilated environmental chamber at 20°C, 80% RH (relative humidity) and atmospheric CO_2 concentration ($\approx$ 400 ppm) for curing. All samples were demoulded as soon as the pastes were stiff enough to hold their shape without the supporting moulds, which occurred after 19 days of curing for prismatic samples, and after 28 days for cylindrical samples. It is likely that such difference across the two types of samples is due to the fact that the prismatic mould exposes a larger surface of the sample to the air and therefore allows a faster drying with respect to the cylindrical samples.

The evolution of the bulk density of curing samples was monitored by taking measurements every 7 days between 21 and 84 days of curing (i.e. the curing ages include testing at 21 days which is a curing time when the specimens were still inside their moulds). Bulk density was calculated using Eq. 1:

$$\rho_b = \frac{W_s}{V_s} \qquad (1)$$

where ρ_b is the bulk density in g/cm^3, W_s is the sample weight in g, and V_s is the sample envelope volume determined using a Vernier calliper.

Changes in the mechanical properties of the hardened samples were monitored overtime by ultrasound pulse velocity (UPV) measurements, three-point bending test and uniaxial compression test. The UPV measurements were carried out on the prismatic samples at the same ages as the bulk density measurements. A Screening Eagle Pundit Lab + portable UPV test instrument was used alongside the software PunditLink, and equipped with 54 kHz Proceq transducers for P-wave measurements, and 40 kHz dry point contact Proceq transducers for S-waves. The ultrasonic pulse velocity was obtained by direct transmission along the x, y and z directions as depicted in Fig. 2. The path lengths along each direction were measured with a Vernier calliper before the analysis. Measurements were taken at the operating conditions of pulse voltage 500 V, probe gain 500×, time frame 0.2 s, pulse width 9.3 μs (for P waves) and 12.5 μs (for S waves). Each measurement was repeated three times and the UPV calculated from the average of the measurements for each direction. The wave travel time was selected manually on the waveform display. The UPV measurements were also used to assess changes in the dynamic Young's modulus overtime as in Nunes et al. [72]. The dynamic Young's modulus (E_d) was calculated from P and S wave velocity measurement data as described in the Supporting Information.
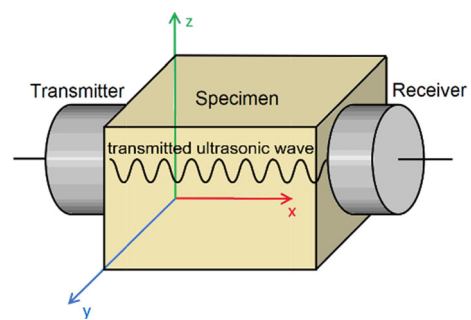

Fig. 2 Schematic illustration of a direct transmission measurement on a $40 \times 40 \times 60$ mm prism specimen for determination of ultrasonic pulse velocity

The three-point bending tests and uniaxial compression tests were performed on the prismatic samples at two ages of 70 and 84 days of curing. Due to the discontinuous nature and to the formation of interfaces in hardening lime pastes, we have decided to monitor the hardening behaviour overtime with UPV, a non-destructive technique, and carry out the compression and flexural strength tests at older ages when the pastes developed sufficient strength to produce reliable data. The compressive test was performed on the broken halves of the prismatic samples used in the flexural tests. The tests were performed with an Ametek Lloyd LR100K Plus testing machine with loading cell of 100 kN capability, and load cell accuracy of 0.5% as described in EN 196-1:2016 [67] at a load rate of 0.2 mm/min and a distance between the two supports of 40 mm.

2.5 Microstructural analysis

Chemical, mineralogical and microstructural characteristics of the hardened pastes were investigated using phenolphthalein, XRD and SEM analyses respectively, at 28, 35, 42, and 56 days of curing on the cylindrical samples. XRD analysis was aimed at assessing the carbonation rate, and performed using a Rigaku SmartLab instrument. The X-ray source was a Cu tube producing K_α radiation, scans were collected in the 10°–90° 2θ range with steps of 0.5° and scan speed of 1°/min, at 50 kV and 40 mA. Data analysis was carried out with the Rigaku SmartLab Studio II software. Phase identification was performed using a search/match approach. Quantitative phase analysis was performed using the Rietveld method implemented in the Rigaku SmartLab Studio II software. The phenolphthalein test was carried out on chisel-split halves of paste specimens using a 1% ethanol solution (indicator grade) from Fisher Scientific, according to EN 14630 [73]. The test surfaces were photographed within 2 s after spraying. SEM images of the hardened pastes were obtained using a Tescan Mira3 microscope in high vacuum mode at 5–15 kV voltage using secondary electrons (SE) signal from both, chamber mounted and in-column SE detectors. Fresh cross sections were obtained by splitting the specimen with a narrow flat chisel or a scalpel. The fragments were carefully dusted with a pressurised nitrogen gun, mounted on a metal stub and fixed with copper conductive tape. The sections were then coated with a 7 nm platinum layer to prevent negative charging of the surfaces and, thus, to investigate their topography (crystal size and shape, micro-cracks, texture). Image analysis was carried out using the software ImageJ v. 1.53a [52].

3 Results

3.1 Fresh-state properties

3.1.1 Water retention tests

The percent change in water retention of the modified samples with respect to the control (ΔWR) is calculated with Eq. 2:

$$\Delta WR = \frac{WR_{sample} - WR_{control}}{WR_{control}} \times 100 \quad (2)$$

where $WR_{control}$ is the water retention of the control sample, and WR_{sample} is the water retention of the sucrose-modified sample. Based on Eq. 2, ΔWR is negative when the paste with the sucrose-modified lime retains less water than the control. Results of the water retention tests of fresh pastes are reported in Table 2, and show that the WR of the sucrose-modified pastes (i.e. S1 and S2) is slightly reduced compared to the control.

3.1.2 Viscosity tests

Results of the viscosity tests are reported in Table 3. The percent change in viscosity of the modified samples with respect to the control (Δη) is calculated using Eq. 3:

$$\Delta\eta = \frac{\eta_{sample} - \eta_{control}}{\eta_{control}} \times 100 \quad (3)$$

Table 2 Water retention of the tested lime pastes

Sample	Water retention, WR (%)	ΔWR (%)
Control	92.5 ± 0.7	N.A
S1	89.9 ± 1.3	− 2.8 ± 0.8
S2	82.9 ± 1.2	− 10.4 ± 0.2

Table 3 Viscosity of the tested lime pastes

Sample	Viscosity η (mPa·s)	$\Delta\eta(\%)$
Control	660 ± 60	N.A
S1	590 ± 10	-11 ± 1
S2	138 ± 2	-79 ± 0.2

where $\eta_{control}$ is the viscosity of the control sample, and η_{sample} is the viscosity of the sucrose-modified sample. The results show that the presence of sucrose decreases the viscosity of the sucrose-modified pastes and that this effect is particularly relevant when sucrose is added after the slaking (sample S2). In sample S2 a 79% reduction was found compared to the control.

3.1.3 Flowability tests

Results of the flowability tests are reported in Table 4. The change in flowability of the modified samples with respect to the control (ΔF) is calculated with Eq. 4:

$$\Delta F = \frac{F_{sample} - F_{control}}{F_{control}} \times 100 \tag{4}$$

where $F_{control}$ is the flowability of the control sample, and F_{sample} is the flowability of the sucrose-modified sample. The results suggest that, consistently with the results of the viscosity test, an increase in flowability was measured in the sucrose-modified pastes, in particular in sample S2 (+75% compared to the control).

3.2 Hardened-state properties

Upon curing, it was observed that a difference in cracking susceptibility was occurring between the different types of paste. Figure 3 shows the samples at

Table 4 Flowability of the tested lime pastes

Sample	Flowability F (mm)	$\Delta F(\%)$
Control	171.1 ± 1.2	N.A
S1	229.0 ± 3.5	33.8 ± 0.1
S2	299.4 ± 1.2	75.0 ± 0.03

70 days of curing, and as seen most of the control specimens had sign of damage, cracks and splitting across the whole section (these samples are high-lighted with a red rectangle in Fig. 3), while only few S1 samples showed cracking and splitting, and none of the S2 samples showed damage or cracking.

3.2.1 UPV tests

Figure 4a shows the results of the UPV measurements at different curing times. Data related to the P-waves of the control sample suggest a small but steady increase in UPV value over the whole testing period, due to the increase in compactness due to the carbonation process. Instead, the same data for S1 and S2 samples suggest that, after the initial 35 days where a significant reduction is observed, the P-waves start to slowly increase overtime at a rate similar to the control. The data also show that the P-wave values for the S2 samples are always higher than that of S1 samples, and very similar to those of the control (whereas the P-waves for the S1 samples are always lower than those of the control).

Results of the bulk density taken at the same times of the UPV measurements are reported in Fig. 4b. Results show that, in the period up to 42 days all three types of paste are subject to a significant decrease in bulk density, which may be attributed to the evapo-ration of the pore water. Such decrease in bulk density is faster in the S1 paste, which reaches a plateau value in 35 days, compared to control and S2, which reach a plateau in 42 days instead.

Figure 5 shows the dynamic Young's modulus determined using the UPV values, at 70 and 84 days. The relative Poisson's ratio values are reported in Table S1 of the Supporting Information. The results show similar moduli across control and S2 pastes, with the mean values of the dynamic Young's moduli in a range between 1.7–2.3 GPa. It is important to note that there was a large scattering of the results of the control and S2 pastes, possibly due to sample inhomogeneity and formation of interfaces between carbonated and non-carbonated areas. The S1 pastes show a lower Young's modulus—1.25 and 1.32 GPa at 70 and 84 days, respectively. The results are in good agree-ment with those obtained by Nezerka [74], who found values of the dynamic Young's moduli of 3.2 GPa in lime mortars at 90 days of curing.
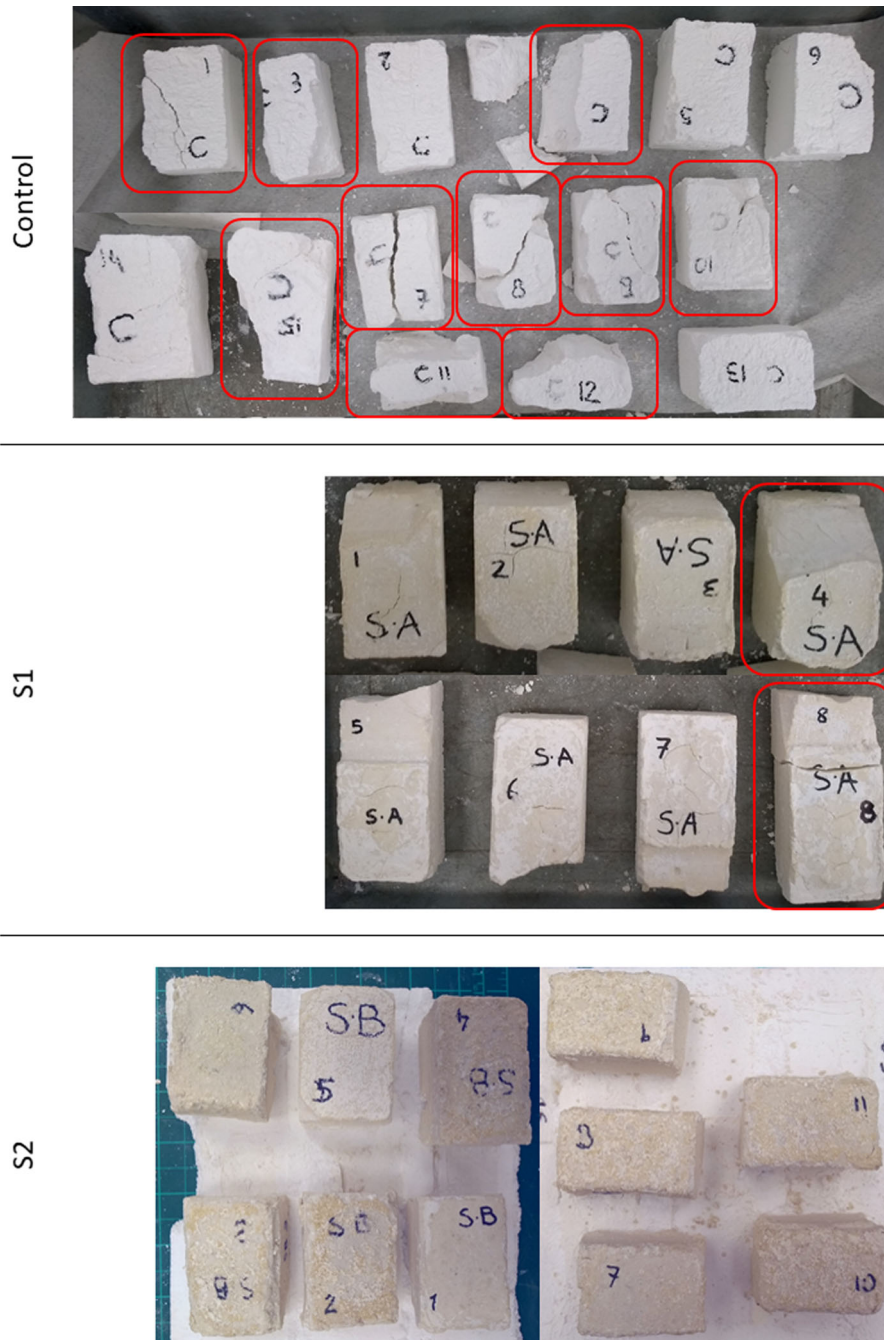
Fig. 3 Lime paste samples at 70 days curing. Control samples show extensive crack formation and damage due to drying shrinkage (samples highlighted by red rectangles). Few S1 samples are cracked or damaged (samples in red rectangles). None of the S2 samples is damaged, and no cracks are observed. (Color figure online)

3.2.2 Flexural tests

Figure 6 shows an S1 paste specimen under testing. Figure 7 shows the results of the three-points bending tests. At 70 days of curing, the pastes show flexural strength in the range 0.05–0.1 MPa. At 84 days the flexural strength of S2 samples (0.23 MPa) is significantly higher than that of the control and S1 pastes
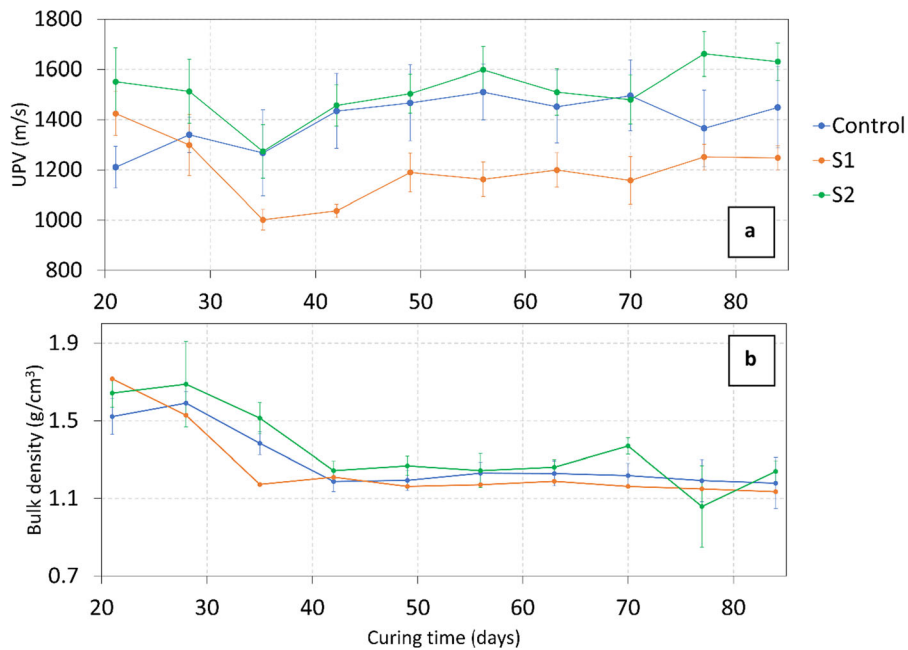
Fig. 4 **a** weekly *P*-waves UPV values and **b** bulk density of control and sucrose-modified lime pastes monitored overtime during curing from 21 to 84 days
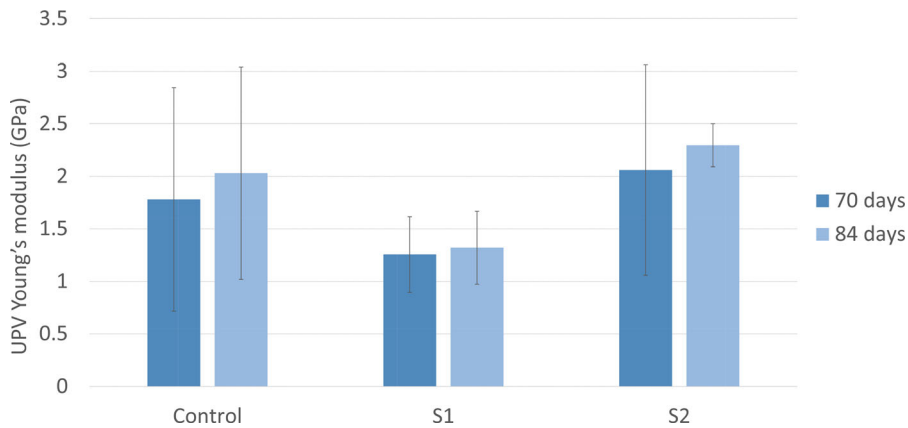

Fig. 5 Young's modulus determined in control and sucrose-modified lime pastes at 70 and 84 days of curing by *P*- and *S*-waves UPV values

(0.12 and 0.07 MPa, respectively). The results suggest that the addition of sucrose after slaking leads to a substantial increase in flexural strength of the lime pastes. A slight increase in flexural strength between 70 and 80 days was measured in the control and S1 pastes.

3.2.3 Compression tests

Figure 8 shows a control paste specimen under testing. Figure 9 shows the results of the uniaxial compression tests. The compressive strength of the three pastes is similar at 70 days of curing, with mean values included between 0.82 and 0.93 MPa. However, an increase in compressive strength is recorded at 84 days of curing for all samples, with compressive strength mean values ranging between 0.99 and
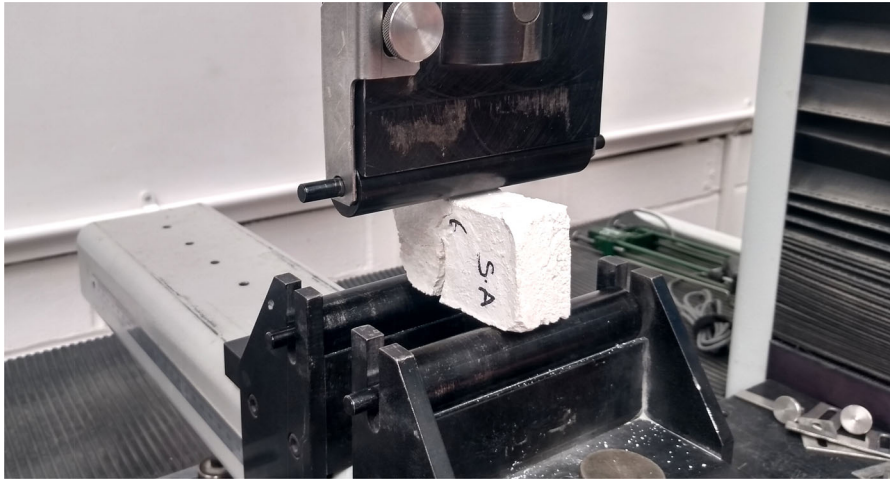
Fig. 6 Set-up of the three-point bending test and typical failure mode of a paste specimen
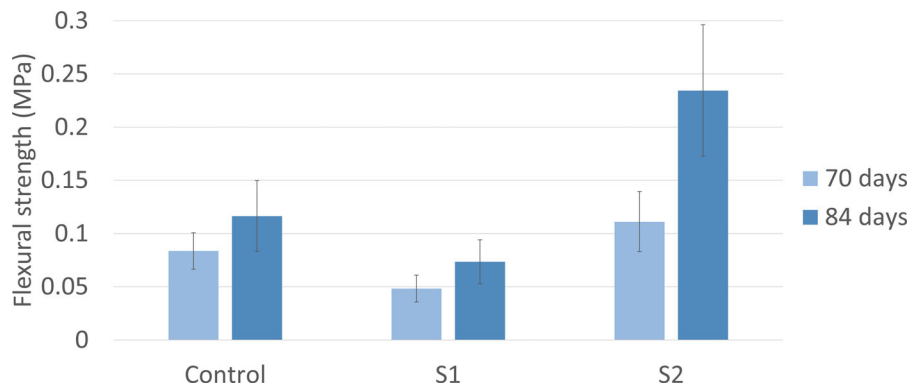

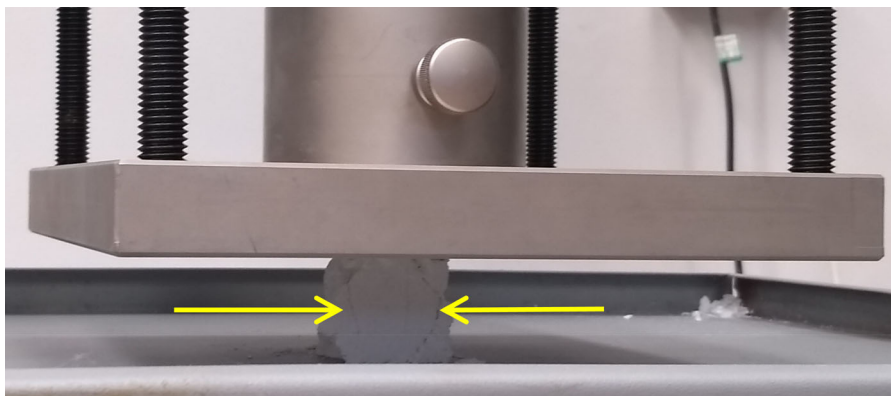**Fig. 7** Flexural strength of control and sucrose-modified lime pastes at 70 and 84 days of curing

Fig. 8 Set-up of the uniaxial compressive test and typical failure mode of a paste specimen. The yellow arrows highlight the cracks originated by the loading
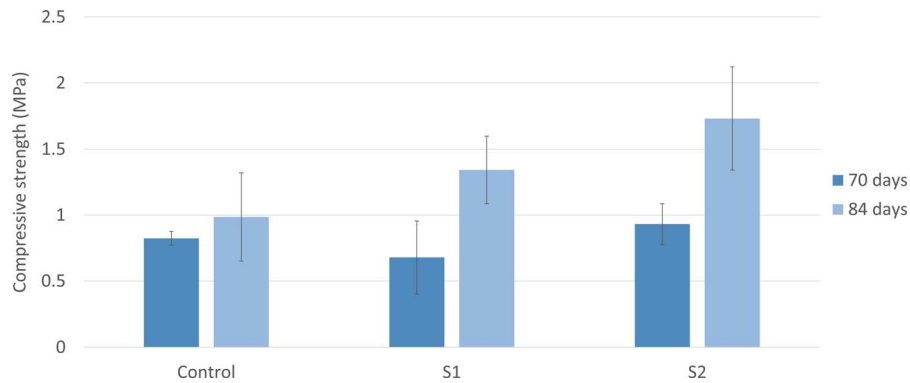
Fig. 9 Compressive strength of control and sucrose-modified lime pastes at 70 and 84 days of curing

1.73 MPa. At this age, a significant difference in strength is recorded across the three pastes. The control paste shows the lowest compressive strength (0.99 MPa mean value), whereas the S1 paste shows a higher mean value (1.34 MPa), and the S2 paste shows the highest compressive strength (1.73 MPa mean value). The results show that the addition of sucrose to lime paste leads to an increase in compressive strength, and that this increase is more marked when sucrose is added after slaking.

3.2.4 Phenolphthalein tests

Figure 10 shows the results of the phenolphthalein tests. The staining of the cross sections for the control paste shows a homogeneous, pink-stained surface at 28 days of curing, suggesting that limited carbonation must have taken place during the first 28 days. At 35 days, a non-stained external ring with depth of about 2 mm appears, suggesting a substantial formation of calcium carbonate. The depth of the rim remained approximately constant up to 56 days of curing, suggesting that between 35 and 56 days the pH of the whole section did not drastically change and that
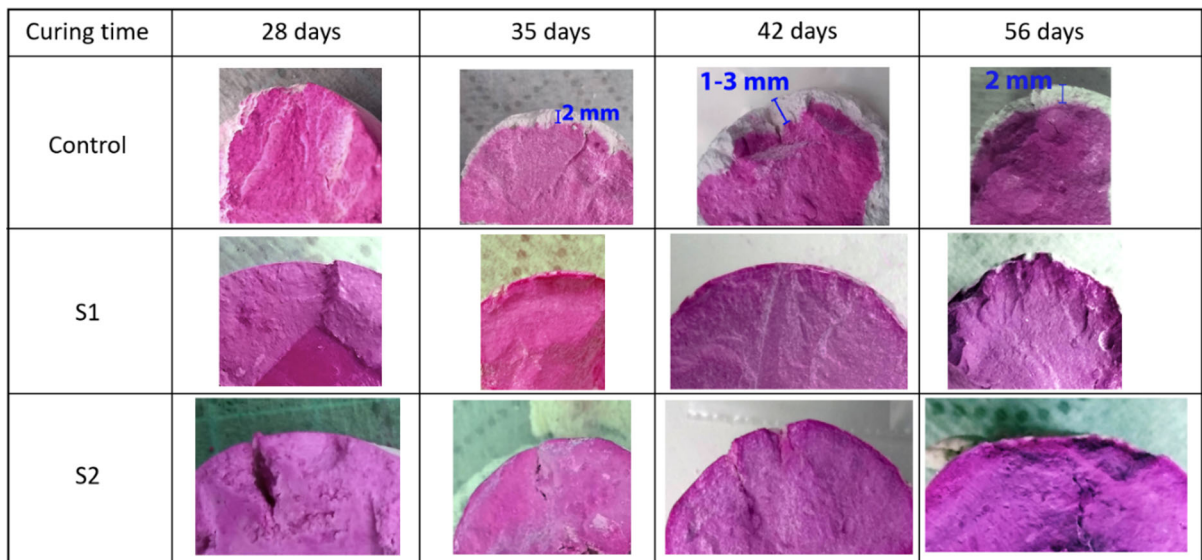

Fig. 10 Photographic records of freshly broken sections of lime paste specimens sprayed with phenolphthalein. Comparison between control, sucrose solution-modified (S1), and solid sucrose-modified (S2) lime pastes at various ages
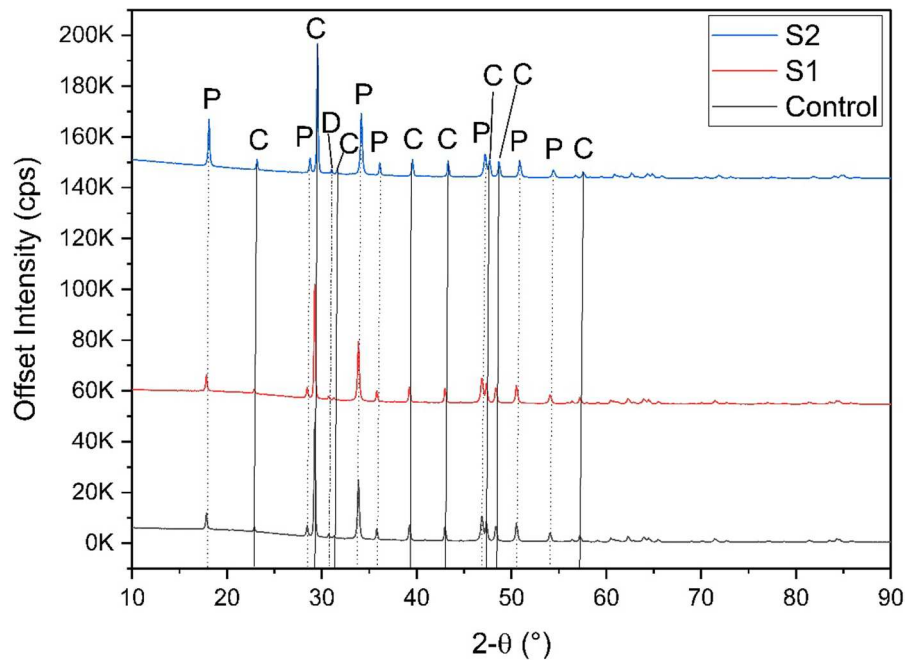
Fig. 11 Diffractograms of the control, S1 and S2 pastes at 28 days of curing. The identified phases are shown with the following keys: *P* portlandite, *C* calcite; *D* dolomite. *Cps* counts per second

therefore the carbonation rate slowed down with respect to the period between 28 and 35 days.

Conversely, the cross sections of sucrose-modified lime pastes showed a homogeneous, pink-stained surface throughout the testing period that is up to 56 days of curing. This suggests that limited carbonation had occurred throughout the whole body of the samples.

3.2.5 XRD analysis

The diffractograms of the control, S1 and S2 pastes at 28 days are shown in Fig. 11. The only identified mineral phases were calcite, portlandite and dolomite. The presence of calcite is due to both, the addition of marble powder as a filler, and the carbonation of lime putty. No other calcium carbonate polymorph could be identified in any of the collected diffractograms. It is likely that the presence of calcite crystals from the marble powder fostered the formation of calcite from the carbonation reaction and, consequently, prevented the formation of other polymorphs of calcium carbonate [75]. The presence of portlandite is due to the uncarbonated lime. The limited amounts (< 2% wt) of dolomite found in the samples were introduced by the

marble powder. No other phases were identified in the samples even at later stages of curing.

The carbonation progress in all samples was estimated through XRD measurements and expressed as the calcite-to-portlandite % content by weight ratio (*C/P*) as shown in Fig. 12. The XRD measurements show that in the control paste a significant increase in *C/P* is measured at 42 days, suggesting that significant carbonation took place at this age. Conversely, at 56 days, the *C/P* ratio is rather stable. In the S1 paste, the calcite content is already almost twice the portlandite content at 28 days, suggesting that S1 paste is more carbonated than the control at the same curing time. Both in the control and the S1 paste, a significant carbonation progression is measured at 42 days. Nonetheless, the carbonation rate in the S1 paste between 35 and 42 days is much higher than the control, and at 56 days, the carbonation progression is further proceeding at a similar rate. In the S2 paste, the *C/P* ratio at 28 days is similar to S1, however, overtime the increase in *C/P* is very small, suggesting that little carbonation took place in S2 paste. At 56 days, the calcite content is still about twice the portlandite content, i.e. slightly lower than the control at the same curing time.
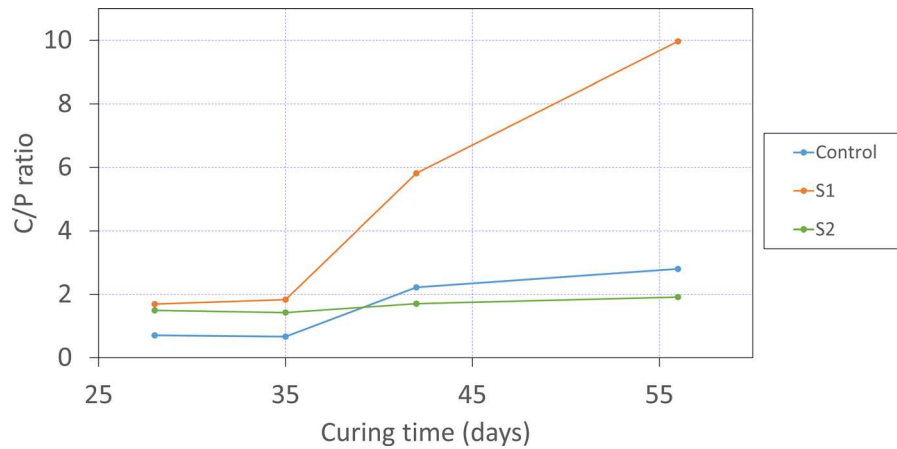
Fig. 12 Graph showing the carbonation progress in control and sucrose-modified lime pastes, estimated by changes overtime of XRD-determined calcite-to-portlandite ratio (C/P)
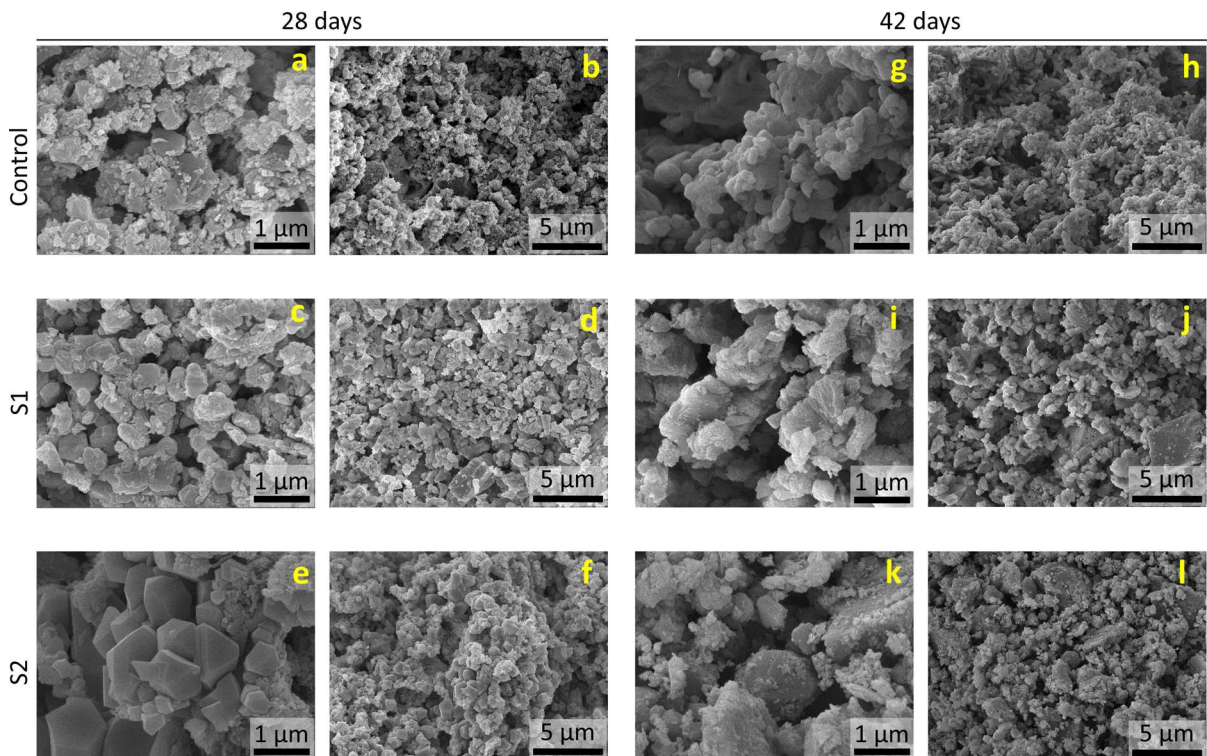

Fig. 13 SEM micrographs of fresh fractures of paste specimens, with and without sucrose additions, at 28 and 42 days of curing. For each curing time, the left column shows a higher magnification and the right column a lower magnification

3.2.6 SEM analysis

A selection of representative images of the microstructures of all pastes at 28 and 42 days of curing is shown in Fig. 13. The images show that at 28 days, several well-developed, hexagonal portlandite crystals in the control paste developed (Fig. 13a), confirming that the binder is still largely uncarbonated. The microstructure appears quite porous, with numerous pores (Fig. 13b). Conversely, the shape of portlandite crystals visible in the S1 and S2 pastes is different from the control, as it is influenced by the presence of sucrose as

shown in a previous study [60]. Portlandite crystals in S1 are of irregular shape and with jagged edges (Fig. 13c), whereas those observed in S2 paste are well-developed and with an elongated prismatic habit (Fig. 13e). Overall, the sucrose-modified pastes show more compact microstructure than the control (Fig. 13d, f). At 35 days, a marked crystal coarsening is observed in S2 paste (Figure SI1 in the Supporting Information) accompanied by the formation of several slit-shaped pores, likely due to drying-induced crystal agglomeration [39] (Figure SI2 in the Supporting Information). The effect of such coarsening can be observed throughout the period of investigation, i.e. both at 42 days (Fig. 13i) and at 56 days (Figure SI3 in the Supporting Information). Signs of partial carbonation can be observed in the control and S2 paste samples, in the form of small calcium carbonate nuclei forming on the surface of portlandite crystals (Figure SI4 in the Supporting Information). A microstructure characterised by agglomerates of scalenohedral calcite crystals can be seen between the areas located near the surface and those in the core of the samples (Fig. 13g, h), which are characterised by a more porous texture and the presence of portlandite crystals (Figure SI5 in the Supporting Information). This confirms the formation of a carbonation crust in the control paste specimens as indicated by the phenolphthalein tests.

4 Discussion

4.1 Effects of sucrose additions on lime paste properties

Results of the water retention tests carried out on the fresh pastes show that sucrose-modified lime pastes retain less water, are less viscous and have a higher flowability compared to the control paste. In particular, minimum water retention, viscosity and maximum flowability are obtained when sucrose is added after the slaking (sample S2). Therefore, the results suggest that sucrose acts as a water-reducing agent, as also recently observed by Kang et al. [2] and explained by the tendency of sucrose to bind with water molecules. The loss in water retention and viscosity and the increase in flowability are a consequence of such high affinity of sucrose for water, which reduces the quantity of water available to bind to portlandite

which would normally form the stiff, water-retentive paste commonly obtained by slaking quicklime with pure water. This appears to be similar to the effect of the addition of sucrose on the rheology of starchy pastes, where it is also observed that sucrose inhibits water activity (and therefore its ability to interact with $Ca(OH)_2$) not only by limiting water availability because of the hydrogen bonding network established with the hydroxyl groups of sucrose, but also by directly interacting with the compounds in the mixture [76].

This study confirms the water-reducing effect already observed in [2] and proves that such effect is drastically enhanced when sucrose is added to the already-slaked lime putty compared to when sucrose is added to the water before the slaking. Arguably, the water-reducing action is not as intense in the S1 paste as in the S2 samples because of the thermal degradation of sucrose when added before slaking for S1 samples, due to the highly exothermal reaction of lime and water (to which S2 was not subject to) as recently discussed by the authors [60]. The high temperature developed during slaking (as high as 200 °C [77]) is likely to lead to the degradation of sucrose molecules through various reaction pathways and eventually to the formation of different species such as monomers glucose and fructose along with other low molecular weight compounds [78]. To this regard, it has been indeed reported that glucose and fructose have a lower capacity to bind water molecules with respect to sucrose [79, 80], which might explain the reduced effects of sucrose in the S1 lime putty.

Therefore, the different properties observed in S1 and S2 lime pastes can be explained as follows. In the S1 lime putty, the presence of sucrose molecules and of their thermal degradation products during slaking can affect the nucleation and growth of portlandite crystals. In turn, the combined effect of the sucrose-modified shape and size of portlandite crystals [60], as well as the presence of sucrose and of its thermal degradation products might hinder the binding of pore water with lime particles resulting in the observed increase in flowability and loss of water retention and viscosity of the lime putty. In the S2 lime putty, the increase in flowability and water retention/viscosity loss occur to a much greater extent due to the higher concentration of sucrose, which did not undergo thermal degradation as in S1, and reduces the formation of lime-water bonds with the consequent result of

impairing the inherently high water retentivity of lime putty [81].

The decreased viscosity and increased flowability observed in the sucrose-modified putties suggest that sucrose acts as a water-reducing agent in a similar way to superplasticisers such as lignosulfonates [82]. Although a high water retention is often regarded as an advantageous property (as it is usually accompanied by a good workability and limited bleeding phenomena), it is also related to a higher risk of crack formation upon drying shrinkage [83]. The empirical observations of our samples throughout the curing period were consistent with the observed fresh properties and, indeed, the susceptibility to cracking and splitting showed the following trend: control $> >$ S1 $>$ S2 (Fig. 3). This observation is also in agreement with the bulk density measurements, which show an initial drastic reduction in bulk density in S2 samples with respect to the control and S1 samples, suggesting a faster initial water loss in S2 samples. This is consistent with an enhanced water-reducing effect of sucrose in S2 samples.

The UPV measurements showed that S2 samples have on average a greater compactness than the control and S1 paste. Several advantageous effects of water-reducing admixtures on the properties of lime mortars have been reported, included allowing a substantial reduction in water content needed to achieve the required consistency, improvement in mechanical strength, while keeping a sufficient porosity and water vapour permeability [84–86], through the use of superplasticizers such as modified lignosulfonates and polycarboxylate ethers. Our UPV results suggest that sucrose, similarly to lignosulfonates, acts as a water-reducing agent and contributes to an increase in compactness of hardened lime pastes, especially if added after the slaking process. The UPV results are in agreement with the results of compression and flexural tests, which show an increase in strength in sucrose-modified lime pastes, especially if sucrose is added after slaking.

Our results of the compression and flexural tests are in good agreement with those obtained by Cizer et al. [22] and Kang et al. [2], who ascribe the strength increase to a higher homogeneity within the load-bearing section of the samples caused by the inhibition of the formation of a carbonation rim due to the presence of sucrose molecules, which is also consistent with our phenolphthalein tests (Fig. 6), although

the carbonation rate can be accelerated or slowed down depending on whether sucrose is added before or after the slaking (Fig. 9).

Remarkably, the combined results of XRD, phenolphthalein and mechanical tests suggest that the degree of conversion of calcium hydroxide into calcium carbonate in a lime paste is not necessarily correlated with an increase in mechanical strength. A similar result was obtained in a previous study [87], where different lime slaking conditions (without use of organic compounds) were tested and the least carbonated lime mortar performed better in terms of compressive and flexural strength than the mortars where carbonation was more advanced.

Results of the microstructural analyses suggest that a carbonation rim developed on the surface of the control paste after 35 days of curing, and such rim seems to act as a passivation layer against further carbonation by limiting new atmospheric CO_2 reacting with lime. The self-limiting character of the carbonation reaction is well known [88–91] and, while it may represent a drawback for the setting of lime mortars, it is instead desirable when the $Ca(OH)_2$ is part of a reinforced concrete, in order to preserve the concrete from excessive acidification and corrosion of rebars [90, 92]. The formation of a passivation layer in the control paste could have been fostered by the coarse microstructure observed at the SEM (Fig. 11b) at 28 days, which allowed for a localised large CO_2 penetration and, in turn, large carbonation of the sample' surface (i.e. the part of the samples immediately exposed to the air). Interestingly, no evidence of the formation of such a passivating layer was found in the sucrose-modified pastes. These results are consistent with the study of Kang et al. [2], who observed a homogeneous and slow carbonation process across the whole section of sucrose-modified lime mortars, in contrast with the rapid and localised carbonation process observed in plain lime mortars. The homogeneous carbonation across the whole body of the specimens of sucrose-modified lime paste revealed by the phenolphthalein test can be partially related to the different microstructure and porosity of samples S1 and S2 compared to the control. These, in fact, are features that are known to affect the evaporation rate of pore water and, in turn, the carbonation of lime mortars [22]. Such differences can be observed in the SEM images, where S1 and S2 pastes show particle coarsening (Fig. 11i,k), while in the control, the micro

texture becomes gradually more compact towards the surface (Fig. 11g), where carbonation takes place first. The textural differences can be related to the different shape and size of portlandite crystals, affected by the presence of sucrose, and to the homogeneous texture of the sucrose-modified pastes conferred by a quasi-monodisperse population of lime particles slaked in sucrose solution, as opposed to the trimodal distribution of plain lime pastes [60].

Test results further show that the addition of sucrose leads to different effects depending on the addition method (i.e. before or after slaking). In particular, carbonation is more advanced in the S1 paste (where sucrose is added to the slaking water before slaking) with respect to the control, whereas it is slightly less advanced than the control in the S2 paste (where sucrose was added after slaking). Remarkably, these trends are only revealed by the XRD measurements through the quantitative analysis of calcite and portlandite content (while the phenolphthalein tests show a homogeneously pink-stained surface in both S1 and S2 pastes, suggesting that carbonation takes place homogenously across the whole sections in both pastes, as previously mentioned). The differences in carbonation progress between S1 and S2 can be explained by two factors.

The first factor is the different composition of the pore water in the two samples, since sucrose is subject to different degradation patterns [60]. In fact, as previously mentioned, when sucrose is added to the slaking water before slaking, sucrose is subject to thermal treatment that leads to the degradation of the molecule into several products (hence the pore water is rich in smaller molecules such as fructose and glucose [60]). When, instead, sucrose is added after slaking, sucrose is not subject to thermal degradation and the pore water is rich in sucrose. The way the different molecules affect the carbonation reaction is still unknown but our data suggest that they may have an effect. It can be speculated that the adsorption of different species on the portlandite crystals and carbonate nuclei can be the reason of the different carbonation rate. Sucrose molecules in the paste S2, may hinder the reaction with CO_2 and, hence, slow down the carbonation reaction [93] whereas, conversely, of the product of the thermal degradation of sucrose in the S1 paste, have a less relevant effect on the carbonation reaction through paths that are yet to be determined but that can be linked with

characteristics like molecular structure, formation of new functional groups, and chemical affinity.

The second factor is the different shape and size of portlandite crystals between S2 and S1 pastes (affected by the presence of sucrose in the former and by sucrose and its thermal degradation by-products in the latter) that affect the carbonation reaction as well. The morphology of portlandite crystals of the paste S1 are characterised by irregular crystal facets [60]. Such habit modification is likely to bring as a consequence a strong increase in specific surface area and, in turn, to promote carbonation as suggested for portlandite habit modifications induced by several organic additives [39, 58]. The correlation between specific surface area and carbonation rate of lime putty is not well-established, but it has been previously proposed in studies investigating the effects of long-term maturation of lime putty [94, 95].

4.2 Implications for the construction industry

Lime-based building materials can cover a wide variety of functions and applications in civil engineering as well as in the conservation of the built heritage, such as bedding mortars for masonries, plasters and renders, repointing, whitewash, finishing mortars, repairs, and flooring [96]. Each of these functions require specific properties in order to optimise the performance of the used mixture. For example, bedding mortars require a certain workability, adequate adhesion to the masonry units, has to be sufficiently strong when set with limited shrinkage, and has to be elastic enough to accommodate movements [20]. Repair mortars, on the other hand, also require compatibility with the original substrate, both in terms of physical–chemical, mechanical, and aesthetic properties [17, 97]. Thus, depending on the final use of a lime-based mixture, several characteristics (selection of raw materials, formulations, type of application, etc.) need to be gauged in order to obtain the desired properties [97, 98].

This study suggests that the mode of addition of sucrose is a critical parameter influencing the properties of the final mixture. Paste S1, produced by dissolving the sucrose in water prior to the lime slaking, exhibits a lower dynamic elastic modulus, a less compact structure and lower mechanical strength with respect to paste S2, produced by adding the sucrose to the already slaked lime putty, which instead

exhibits a greater mechanical strength and higher compactness. Therefore, pastes of type S1 can be advantageous if applied when greater elasticity is needed, e.g. a bedding mortar in a masonry where movements are likely to occur as a result of creep or thermal effects [20]. Moreover, S1 paste showed to carbonate much faster than S2, therefore it can be advantageous for outdoor applications such as renders and plasters, where rainy weather conditions can impair the quality of the work especially at the very early stage, when lime-based materials are still rather water-soluble [99] and the mechanical properties are not a major issue. An S1-like mortar can show advantageous properties in such applications with respect to plain lime-based mixtures as its workability is slightly improved while carbonation occurs in a homogeneous manner throughout its depth, avoiding the formation of an outer carbonated crust which can readily detach [94]. The properties of the S1 paste are likely to be conferred by the different portlandite crystallisation pathway that occurs when lime is slaked in presence of sucrose and that leads to the formation of smaller, mono-disperse crystals and an overall finer micro texture [2, 39, 60] and such microstructural features are likely to make the $Ca(OH)_2$ more prone to carbonation [100]. Conversely, the S2 paste prepared in this study exhibits big, well-developed portlandite crystals [60] whose high lattice order and crystallinity is likely to contribute to the greater compactness and higher mechanical strength observed in this study. This type of lime-based materials can be advantageous when used for applications where an adequate mechanical performance is required, e.g. repair mortars [14, 36].

5 Conclusions

This research shows that sucrose affects the fresh properties of lime-based pastes as well as those of the hardened samples. In particular, sucrose lowers water retention of the pastes, reduces their viscosity and increases the flowability. The effects are more marked when sucrose is added after slaking (sample S2) rather than before (sample S1), because of the higher concentration of sucrose molecules—responsible for the effects—in sample S2 due to the lack of thermal degradation of sucrose (characteristic of the process in S1). Overall, our results indicate that sucrose acts as a

water-reducing agent with more marked effect when added after slaking.

During curing, sucrose prevents the formation of a passivating layer of $CaCO_3$ at the interface between the sample and the surrounding air. The addition mode of sucrose (before or after slaking) results in different carbonation rates of the pastes: S1 pastes carbonate faster than the control, whereas S2 pastes carbonate slower than the control. Such difference is likely caused by different portlandite crystals morphology, and/or by the presence of different organic species (sucrose in S2 paste; thermal degradation by-products in S1 paste) adsorbed onto $Ca(OH)_2$ particles, and by the different porosity. Mechanical tests suggest that the S2 pastes are more compact and stronger both, in compression and in flexure than the control and the S1 paste.

Future research should investigate the effects of sucrose and its degradation products at various concentrations to identify the best concentration that maximises the properties above mentioned. Furthermore, it is worth noting that the presence of sucrose in a lime mortar might promote biodegradation as this organic compound is known to promote fungal growth and growth of other microorganisms and, in doing so, it promotes several biodegradation pathways [101, 102]. It should be then investigated the durability of sucrose-modified lime mixtures in order to promote their use in the construction industry.

Declarations

References

1. Ritchie H, Roser M (2020) Emissions by sector. In: CO2 GHG Emiss. database. ourworldindata.org/emissions-by-sector. Accessed 13 May 2021

2. Kang SH, Kwon YH, Moon J (2020) Controlling the hydration and carbonation in lime-based materials: advantage of slow carbonation in CO2 curable construction materials. Constr Build Mater 249:118749. https://doi.org/10.1016/j.conbuildmat.2020.118749

3. Provis JL, Bernal SA (2014) Geopolymers and related alkali-activated materials. Annu Rev Mater Res 44:299–327. https://doi.org/10.1146/annurev-matsci-070813-113515

4. Provis JL (2018) Alkali-activated materials. Cem Concr Res 114:40–48. https://doi.org/10.1016/j.cemconres.2017.02.009

5. Oey T, Kumar A, Bullard JW et al (2013) The filler effect: the influence of filler content and surface area on cementitious reaction rates. J Am Ceram Soc 96:1978–1990. https://doi.org/10.1111/jace.12264

6. Scrivener K, Martirena F, Bishnoi S, Maity S (2018) Calcined clay limestone cements (LC3). Cem Concr Res 114:49–56. https://doi.org/10.1016/j.cemconres.2017.08.017

7. Hansen EF, Rodríguez-Navarro C, Balen K (2008) Lime putties and mortars. Stud Conserv 53:9–23. https://doi.org/10.1179/sic.2008.53.1.9

8. Moropoulou A, Bakolas A, Aggelakopoulou E (2001) The effects of limestone characteristic, granulation and calcination temperature to the reactivity of quicklime. Cem Concr Res 31:633–639

9. Cazalla O, Rodriguez-Navarro C, Sebastian E, Cultrone G (2000) Effects on traditional lime mortar carbonation. J Am Ceram Soc 83:1070–1076

10. Rodriguez-Navarro C, Hansen E, Ginell WS (1998) Calcium hydroxide crystal evolution upon aging of lime putty. J Am Ceram Soc 81:3032–3034. https://doi.org/10.1111/j.1151-2916.1998.tb02735.x

11. Elert K, Rodriguez-Navarro C, Pardo ES et al (2002) Lime mortars for the conservation of historic buildings. Stud Conserv 47:62–75. https://doi.org/10.1179/sic.2002.47.1.62

12. Cultrone G, Sebastián E, Huertas MO (2005) Forced and natural carbonation of lime-based mortars with and without additives: mineralogical and textural changes. Cem Concr Res 35:2278–2289. https://doi.org/10.1016/j.cemconres.2004.12.012

13. Cizer Ö, Rodriguez-Navarro C, Ruiz-Agudo E et al (2012) Phase and morphology evolution of calcium carbonate precipitated by carbonation of hydrated lime. J Mater Sci 47:6151–6165. https://doi.org/10.1007/s10853-012-6535-7

14. Moropoulou A, Bakolas A, Moundoulas P et al (2005) Strength development and lime reaction in mortars for repairing historic masonries. Cem Concr Compos 27:289–294. https://doi.org/10.1016/j.cemconcomp.2004.02.017

15. Lawrence M (2006) A study of carbonation in non-hydraulic lime mortars. University of Bath

16. Ventolà L, Vendrell M, Giraldez P, Merino L (2011) Traditional organic additives improve lime mortars: new old materials for restoration and building natural stone fabrics. Constr Build Mater 25:3313–3318. https://doi.org/10.1016/j.conbuildmat.2011.03.020

17. Lanas J, Alvarez JI (2003) Masonry repair lime-based mortars: factors affecting the mechanical behavior. Cem Concr Res 33:1867–1876. https://doi.org/10.1016/S0008-8846(03)00210-2

18. Martínez-Ramírez S, Puertas F, Blanco-Varela MT et al (1998) Behaviour of repair lime mortars by wet deposition process. Cem Concr Res 28:221–229. https://doi.org/10.1016/S0008-8846(97)00262-7

19. Ball RJ, Molinari M, Grant J, Parker SC (2016) Atomistic modelling for the study of dissolution and carbonation of lime. In: 36th cement and concrete science conference. Cardiff

20. Hendry EAW (2001) Masonry walls: materials and construction. Constr Build Mater 15:323–330. https://doi.org/10.1093/elt/ccx019

21. Rosson BT, Søyland K, Boothby TE (1998) Inelastic behavior of sand-lime mortar joint masonry arches. Eng Struct 20:14–24. https://doi.org/10.1016/S0141-0296(97)00052-7

22. Cizer Ö, Ruiz-Agudo E, Rodriguez-Navarro C (2018) Kinetic effect of carbonic anhydrase enzyme on the carbonation reaction of lime mortar. Int J Archit Herit 12:779–789. https://doi.org/10.1080/15583058.2017.1413604

23. Smith AS (2016) Freeze-thaw durability of cement-lime-sand mortars. In: Brick block mason trends, Innov challenges: Proceedings 16th international brick, block, masonry conference IBMAC 2016, pp 547–554

24. Klemm AJ, Wiggins DE (2015) Lime mortar and sacrificial protection of heritage stonework. Proc Inst Civ Eng: Eng Hist Herit 168:167–176. https://doi.org/10.1680/jenhh.15.00013

25. Wiggins D, Ph H, Mice DI (2018) Functional behaviour of traditional Lime Mortar

26. De Nardi C, Cecchi A, Ferrara L et al (2017) Effect of age and level of damage on the autogenous healing of lime mortars. Compos Part B Eng 124:144–157. https://doi.org/10.1016/j.compositesb.2017.05.041

27. Auvinen J, Wirtanen L (2008) The influence of photocatalytic interior paints on indoor air quality. Atmos Environ 42:4101–4112. https://doi.org/10.1016/j.atmosenv.2008.01.031

28. Maskell D, Ferreira Pinto Da Silva C, Mower K, et al (2017) Bio-based plaster for improved indoor air quality.

In: International Conference on bio-based building materials. Clermont-Ferrand

29. Shirakawa MA, Beech IB, Tapper R et al (2003) The development of a method to evaluate bioreceptivity of indoor mortar plastering to fungal growth. Int Biodeterior Biodegrad 51:83–92. https://doi.org/10.1016/S0964-8305(01)00129-9

30. Fourmentin M, Faure P, Gauffinet S et al (2015) Porous structure and mechanical strength of cement-lime pastes during setting. Cem Concr Res 77:1–8. https://doi.org/10.1016/j.cemconres.2015.06.009

31. Ismael NS, Ghanim MN (2015) Properties of blended cement using metakaolin and hydrated lime. Adv Cem Res 27:321–328. https://doi.org/10.1680/adcr.14.00003

32. Kuparinen K, Vakkilainen E (2017) Green pulp mill: renewable alternatives to fossil fuels in lime kiln operations. BioResources 12:4031–4048. https://doi.org/10.15376/biores.12.2.4031-4048

33. Hart PW (2020) Alternative "green" lime kiln fuels: part ii—woody biomass, bio-oils, gasification, and hydrogen. Tappi J 19:271–279. https://doi.org/10.32964/TJ19.5.271

34. Francey S, Tran H, Berglin N (2011) Global survey on lime kiln operation, energy consumption, and alternative fuel usage. Tappi J 10:19–26. https://doi.org/10.32964/tj10.8.19

35. Tregambi C, Solimene R, Montagnaro F et al (2018) Solar-driven production of lime for ordinary Portland cement formulation. Sol Energy 173:759–768. https://doi.org/10.1016/j.solener.2018.08.018

36. Arandigoyen M, Alvarez JI (2007) Pore structure and mechanical properties of cement–lime mortars. Cem Concr Res 37:767–775. https://doi.org/10.1016/j.cemconres.2007.02.023

37. Sébaïbi Y, Dheilly RM, Beaudoin B, Quéneudec M (2006) The effect of various slaked limes on the microstructure of a lime-cement-sand mortar. Cem Concr Res 36:971–978

38. Ergenç D, Fort R (2018) Accelerating carbonation in lime-based mortar in high CO_2 environments. Constr Build Mater 188:314–325. https://doi.org/10.1016/j.conbuildmat.2018.08.125

39. Rodriguez-navarro C, Burgos-cara A, Di LF et al (2020) Nonclassical crystallization of calcium hydroxide via amorphous precursors and the role of additives. Cryst Growth Des. https://doi.org/10.1021/acs.cgd.0c00241

40. Colombo A, Geiker MR, Justnes H et al (2017) On the effect of calcium lignosulfonate on the rheology and setting time of cement paste. Cem Concr Res 100:435–444. https://doi.org/10.1016/j.cemconres.2017.06.009

41. Pesce C, Pesce GL (2020) Effect of lignosulfonates on the morphology of calcium hydroxide crystals. In: 40th cement and concrete science conference. Rilem, Sheffield

42. Yang F, Zhang B, Ma Q (2010) Study of sticky rice: lime mortar technology for the restoration of historical masonry construction. Acc Chem Res 43(6):936–944

43. El-Turki A, Ball RJ, Wang CF, Allen GC (2005) A study of novel lime based mortars consisting of lime, oyster shell lime, clay, sugar, sand and rice using focused ion beam microscopy, Raman spectroscopy and mechanical testing. In: 10th euroseminar on microscopy applied to building materials. Paisley

44. Zhao P, Jackson MD, Zhang Y et al (2015) Material characteristics of ancient Chinese lime binder and experimental reproductions with organic admixtures. Constr Build Mater 84:477–488. https://doi.org/10.1016/j.conbuildmat.2015.03.065

45. Fang SQ, Zhang H, Zhang BJ, Zheng Y (2014) The identification of organic additives in traditional lime mortar. J Cult Herit 15:144–150. https://doi.org/10.1016/j.culher.2013.04.001

46. Li J, Zhang B (2019) Why ancient Chinese people like to use organic-inorganic composite mortars?: application history and reasons of organic-inorganic mortars in ancient Chinese buildings. J Archaeol Method Theory 26:502–536. https://doi.org/10.1007/s10816-018-9380-4

47. Carran D, Hughes J, Leslie A, Kennedy C (2012) A short history of the use of lime as a building material beyond Europe and North America. Int J Archit Herit 6:117–146. https://doi.org/10.1080/15583058.2010.511694

48. Cowper AD (1927) Lime and lime mortars. Building Research Station

49. Centauro I, Cantisani E, Grandin C et al (2017) The influence of natural organic materials on the properties of traditional lime-based mortars. Int J Archit Herit 11:670–684. https://doi.org/10.1080/15583058.2017.1287978

50. Thirumalini P, Ravi R, Sekar SK, Nambirajan M (2011) Study on the performance enhancement of lime mortar used in ancient temples and monuments in India. Indian J Sci Technol 4:1484–1487. https://doi.org/10.17485/ijst/2011/v4i11/30275

51. Ravi R, Rajesh M, Thirumalini S (2018) Mechanical and physical properties of natural additive dispersed lime. J Build Eng 15:70–77. https://doi.org/10.1016/j.jobe.2017.10.009

52. Thirumalini S, Ravi R, Rajesh M (2018) Experimental investigation on physical and mechanical properties of lime mortar: effect of organic addition. J Cult Herit 31:97–104. https://doi.org/10.1016/j.culher.2017.10.009

53. Martínez-Ramírez S, Higueruela LR, Cascales I et al (2019) New approach to nanolime synthesis at ambient temperature. SN Appl Sci 1:1–8. https://doi.org/10.1007/s42452-018-0122-8

54. Milestone NB (1979) Hydration of tricalcium silicate in the presence of lignosulfonates, glucose, and sodium gluconate. J Am Ceram Soc 62:321–324. https://doi.org/10.1111/j.1151-2916.1979.tb19068.x

55. Young JF (1972) A review of the mechanisms of set-retardation in portland cement pastes containing organic admixtures. Cem Concr Res 2:415–433. https://doi.org/10.1016/0008-8846(72)90057-9

56. Banfill PFG (1986) Precipitation of calcium hydroxide in the presence of organic compounds. J Mater Sci Lett 5:33–34. https://doi.org/10.1007/BF01671426

57. Pannetier N, Khoukh A, François J (2001) Physico-chemical study of sucrose and calcium ions interactions in alkaline aqueous solutions. Macromol Symp 166:203–208. https://doi.org/10.1017/CBO9781107415324.004

58. Rodriguez-Navarro C, Ruiz-Agudo E, Burgos-Cara A et al (2017) Crystallization and colloidal stabilization of $Ca(OH)_2$ in the presence of nopal juice (Opuntia ficus indica): implications in architectural heritage

conservation. Langmuir 33:10936–10950. https://doi.org/10.1021/acs.langmuir.7b02423

59. Tzilivakis J, Jaggard K, Lewis KA et al (2005) Environmental impact and economic assessment for UK sugar beet production systems. Agric Ecosyst Environ 107:341–358. https://doi.org/10.1016/j.agee.2004.12.016

60. Pesce C, Pesce GL, Molinari M, Richardson A (2021) Effects of organic additives on calcium hydroxide crystallisation during lime slaking. Cem Concr Res. https://doi.org/10.1016/j.cemconres.2020.106254

61. Garcia-Carmona J, Gomez-Morales J, Fraile-Sainz J, Rodriguez-Clemente R (2003) Morphological characteristics and aggregation of calcite crystals obtained by bubbling CO_2 through a $Ca(OH)(2)$ suspension in the presence of additives. Powder Technol 130:307–315. https://doi.org/10.1016/S0032-5910(02)00209-7

62. EN 459-1 (2015) Building lime. Definitions, specifications and conformity criteria

63. Doglioni F, Scappin L, Squassina A, Trovò A (2017) Conoscenza e restauro degli intonaci e delle superfici murarie esterne di Venezia. Campionature, esemplificazioni, indirizzi di intervento. Il prato, Venezia

64. Rodriguez-Navarro C, Ruiz-Agudo E, Ortega-Huertas M, Hansen E (2005) Nanostructure and irreversible colloidal behavior of $Ca(OH)_2$: implications in cultural heritage conservation. Langmuir 21:10948–10957. https://doi.org/10.1021/la051338f

65. Rosell JR, Haurie L, Navarro A, Cantalapiedra IR (2014) Influence of the traditional slaking process on the lime putty characteristics. Constr Build Mater 55:423–430. https://doi.org/10.1016/j.conbuildmat.2014.01.007

66. Navrátilová E, Tihlaříková E, Neděla V et al (2017) Effect of the preparation of lime putties on their properties. Sci Rep 7:1–9. https://doi.org/10.1038/s41598-017-17527-3

67. EN 196-1:2016 Methods of testing cement

68. EN 12350-5:2019 Testing fresh concrete: flow table test. 18

69. Hydramotion Ltd (2013) Viscolite 700: VL7. Portable viscometer user manual

70. BS EN 459-2: (2010) BSI standards publication building lime part 2: test methods

71. Hendrickx R, Minet J, Van Balen K, Van Gemert D (2008) Workability of mortars with building lime: assessment by a panel of masons versus lab testing. In: International brick & block masonry conference

72. Nunes C, Slížková Z, Stefanidou M, Němeček J (2016) Microstructure of lime and lime-pozzolana pastes with nanosilica. Cem Concr Res 83:152–163. https://doi.org/10.1016/j.cemconres.2016.02.004

73. European Standard (2006) Products and systems for the protection and repair of concrete structures: Test methods—etermination of carbonation depth in hardened concrete by the phenolphthalein method. EN 14630–2006

74. Nezerka V (2013) Comprehensive study on microstructure and mechanical properties of Lime-Pozzolan pastes

75. Meldrum FC, Colfen H (2008) Controlling mineral {morphologies} and structures in biological and synthetic {systems}. Chem Rev 108:4332–4432. https://doi.org/10.1021/cr8002856

76. Salvador A, Sanz T, Fiszman SM (2006) Dynamic rheological characteristics of wheat flour–water doughs. Effect of adding NaCl, sucrose and yeast. Food Hydrocoll 20:780–786. https://doi.org/10.1016/j.foodhyd.2005.07.009

77. Boynton RS (1980) Chemistry and technology of lime and limestone. Wiley, New York

78. Šimkovic I, Šurina I, Vričan M (2003) Primary reactions of sucrose thermal degradation. J Anal Appl Pyrolys 70:493–504. https://doi.org/10.1016/S0165-2370(03)00007-X

79. Zhang X, Tong Q, Zhu W, Ren F (2013) Pasting, rheological properties and gelatinization kinetics of tapioca starch with sucrose or glucose. J Food Eng 114:255–261. https://doi.org/10.1016/j.jfoodeng.2012.08.002

80. Psimouli V, Oreopoulou V (2012) The effect of alternative sweeteners on batter rheology and cake properties. J Sci Food Agric 92(99):105. https://doi.org/10.1002/jsfa.4547

81. Izaguirre A, Lanas J, Álvarez JI (2009) Effect of water-repellent admixtures on the behaviour of aerial lime-based mortars. Cem Concr Res 39:1095–1104. https://doi.org/10.1016/j.cemconres.2009.07.026

82. Pérez-Nicolás M, Duran A, Navarro-Blasco I et al (2016) Study on the effectiveness of PNS and LS superplasticizers in air lime-based mortars. Cem Concr Res 82:11–22. https://doi.org/10.1016/j.cemconres.2015.12.006

83. Izaguirre A, Lanas J, Álvarez JI (2011) Characterization of aerial lime-based mortars modified by the addition of two different water-retaining agents. Cem Concr Compos 33:309–318. https://doi.org/10.1016/j.cemconcomp.2010.09.008

84. Silva BA, Ferreira Pinto AP, Gomes A, Candeias A (2021) Short- and long-term properties of lime mortars with water-reducers and a viscosity-modifier. J Build Eng 43:103086. https://doi.org/10.1016/j.jobe.2021.103086

85. Fernández JM, Duran A, Navarro-Blasco I et al (2013) Influence of nanosilica and a polycarboxylate ether superplasticizer on the performance of lime mortars. Cem Concr Res 43:12–24. https://doi.org/10.1016/j.cemconres.2012.10.007

86. Vyšvařil M, Žižlavský T (2017) Effect of chitosan ethers on fresh state properties of lime mortars. IOP Conf Ser Mater Sci Eng 251:12039. https://doi.org/10.1088/1757-899x/251/1/012039

87. Pesce C, Godina MC, Henry A, Pesce G (2021) Towards a better understanding of hot-mixed mortars for the conservation of historic buildings: the role of water temperature and steam during lime slaking. Herit Sci 9:1–18. https://doi.org/10.1186/s40494-021-00546-9

88. Cizer Ö, Van Balen K, Elsen J, Van Gemert D (2012) Real-time investigation of reaction rate and mineral phase modifications of lime carbonation. Constr Build Mater 35:741–751. https://doi.org/10.1016/j.conbuildmat.2012.04.036

89. Dheilly RM, Tudo J, Queneudec M (2002) Influence of storage conditions on the carbonation of powdered Ca$(OH)_2$. Constr Build Mater 16:155–161

90. Galan I, Glasser FP, Baza D, Andrade C (2015) Assessment of the protective effect of carbonation on portlandite crystals. Cem Concr Res 74:68–77. https://doi.org/10.1016/j.cemconres.2015.04.001

91. Ruiz-Agudo E, Kudłacz K, Putnis CV et al (2013) Dissolution and carbonation of portlandite [Ca$(OH)_2$] single

crystals. Environ Sci Technol 47:11342–11349. https://doi.org/10.1021/es402061c

92. Woyciechowski P, Woliński P, Adamczewski G (2019) Prediction of carbonation progress in concrete containing calcareous fly ash co-binder. Mater 12:2665

93. Cheung J, Jeknavorian A, Roberts L, Silva D (2011) Impact of admixtures on the hydration kinetics of Portland cement. Cem Concr Res 41:1289–1309. https://doi.org/10.1016/j.cemconres.2011.03.005

94. Van Balen K (2005) Carbonation reaction of lime, kinetics at ambient temperature. Cem Concr Res 35:647–657. https://doi.org/10.1016/j.cemconres.2004.06.020

95. Rodriguez-Navarro C, Cazalla O, Elert K, Sebastian E (2002) Liesegang pattern development in carbonating traditional lime mortars. Proc R Soc A Math Phys Eng Sci 458:2261–2273. https://doi.org/10.1098/rspa.2002.0975

96. Alvarez JI, Veiga R, Martínez-Ramírez S et al (2021) RILEM TC 277-LHS report: a review on the mechanisms of setting and hardening of lime-based binding systems. Mater Struct Constr. https://doi.org/10.1617/s11527-021-01648-3

97. Rodríguez-Navarro C (2012) Binders in historical buildings: traditional lime in conservation. Semin SEM 9:91–112

98. Veiga R (2017) Air lime mortars: what else do we need to know to apply them in conservation and rehabilitation interventions? A review. Constr Build Mater 157:132–140. https://doi.org/10.1016/j.conbuildmat.2017.09.080

99. Fusade L, Orr SA, Wood C et al (2019) Drying response of lime-mortar joints in granite masonry after an intense rainfall and after repointing. Herit Sci 7:38. https://doi.org/10.1186/s40494-019-0277-7

100. Beruto D, Barco L, Belleri G, Searcy AW (1981) Vapor-phase hydration of submicrometer CaO particles. J Am Ceram Soc 64:74–80. https://doi.org/10.1111/j.1151-2916.1981.tb09579.x

101. George RP, Ramya S, Ramachandran D, KamachiMudali U (2013) Studies on biodegradation of normal concrete surfaces by fungus Fusarium sp. Cem Concr Res 47:8–13. https://doi.org/10.1016/j.cemconres.2013.01.010

102. Ryparová P, Wasserbauer R, Rácová Z (2016) The cause of occurrence of microorganisms in civil engineering and the dangers associated with their growth. Proc Eng 151:300–305. https://doi.org/10.1016/j.proeng.2016.07.402